Vortex Interactions and Barotropic Aspects of Concentric Eyewall Formation



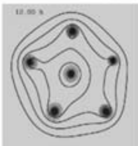

Hung-Chi Kuo

National Chair Professor
Department of Atmospheric Sciences
National Taiwan University
Taipei, Taiwan

University of California Davis

May 7 2010

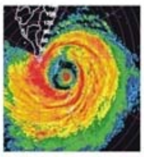
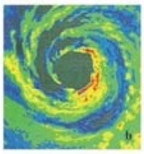
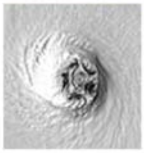

象神颱風侵襲後的台北市 Taipei city aftermath of typhoon

納莉颱風（2001）

桃芝颱風（2001）

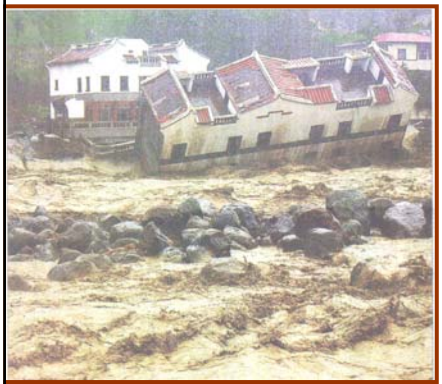

Before

Aftermath

Typhoon Morakot 2009

The Downstream Influences of the Extratropical Transition of Tropical Cyclones

Patrick Harr
Naval Postgraduate School

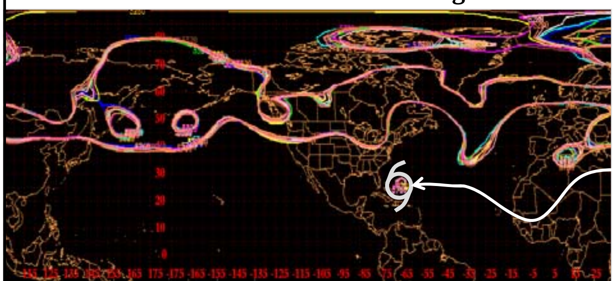

0000 UTC 16 Sep 2003
GFS Ensembles +00

Hurricane Isabel

GFS 500 hPa Ensembles
+108 h
VT 1200 UTC 20 Sep 03

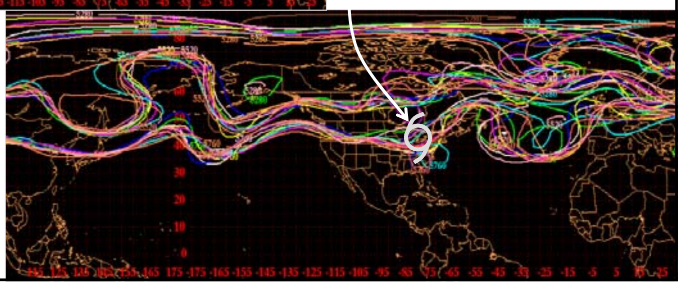

Acknowledgment: Office of Naval Research, Marine Meteorology Program

West Pac Track Errors cut in half since 1990

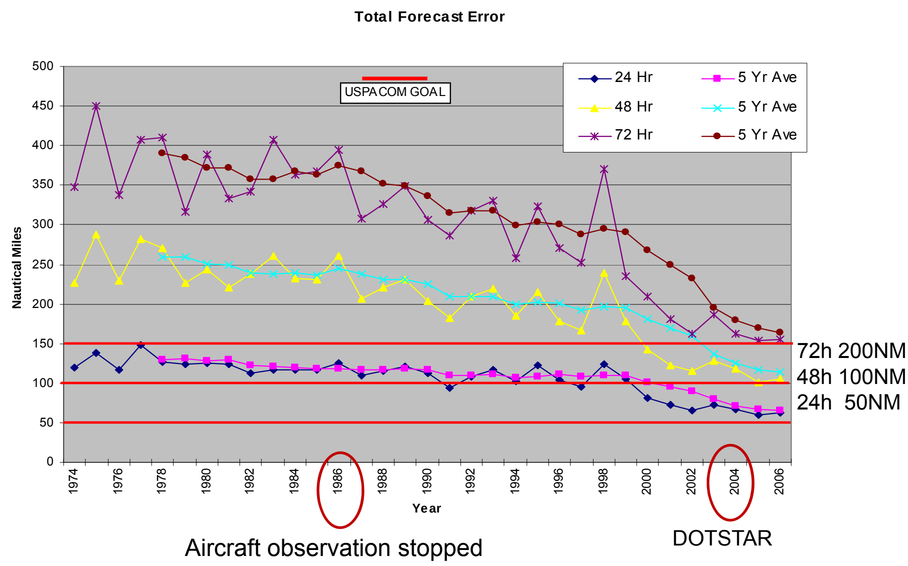

Edward Fukada

JTWC

Error cut in half since 1990

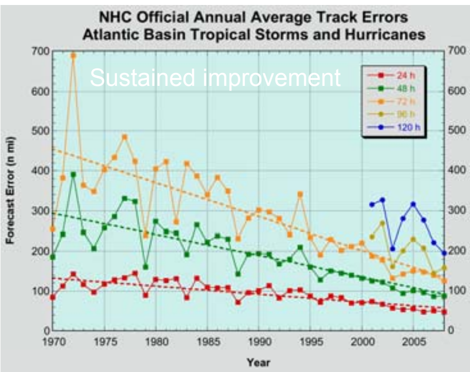

No progress in the last 20 years

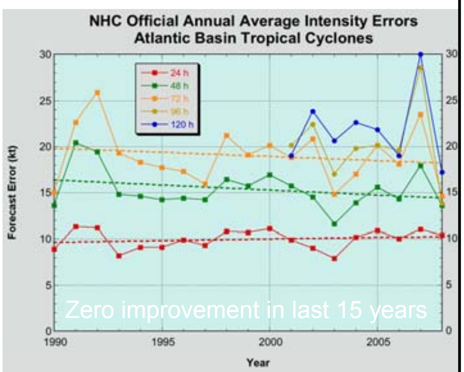

www.nhc.noaa.gov/verification/verify5.shtml

Why such a big difference between track and intensity?

Courtesy of Dr. G. Holland

Environmental Factors

Typhoon weakens
over region of cold water or low ocean heat content,
over land or region of decreased humidity,
over region of strong vertical wind shear.

However, the variance of typhoon intensity change from climatology is not explained well by the synoptic-scale environmental conditions.

It is fairly typical for typhoons to strengthen or weakens rapidly without any clear commensurate changes in the environment.

Internal meso-scale processes matter!

Latent Heat during typhoon made landfall

Precipitation ~1600*mm*

$1600\ mm = 1.6\ m$

$1.6\ m * 1000\ kg\ m^{-3} * 2.5\times10^{6}\ J\ kg^{-1}$

$= 4 \times 10^{9}\ J\ m^{2}$

$4\times10^{9}\ J\ m^{2} * 2.5\times10^{9}\ m^{2}\ \sim10^{19} J$

Annual energy usage in Taiwan 10^{17}J

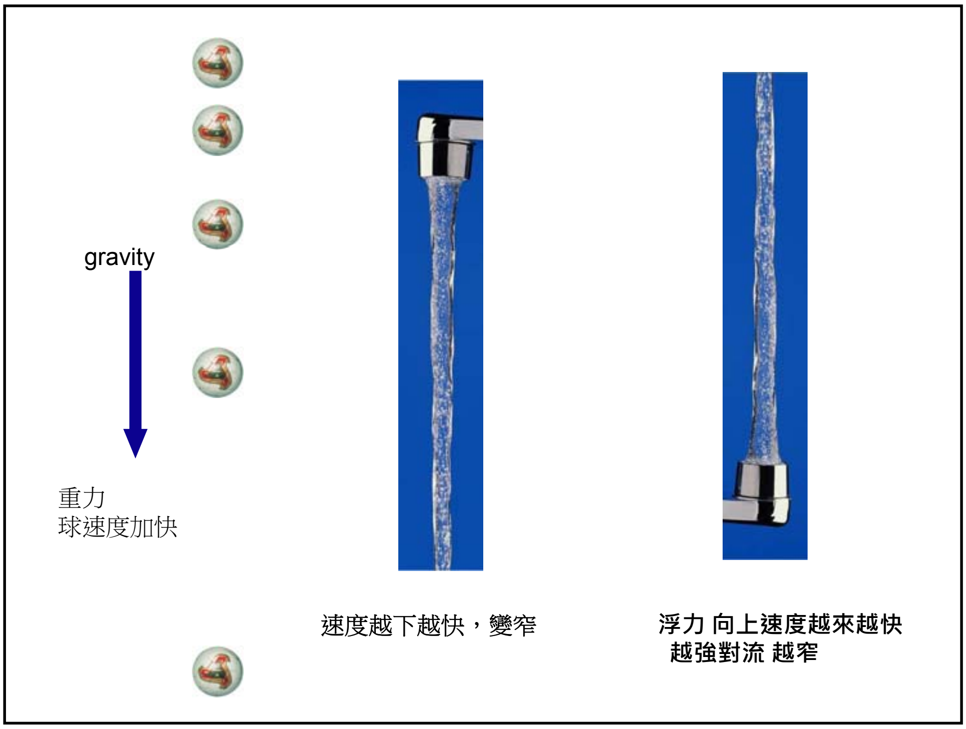
gravity
重力
球速度加快
速度越下越快，變窄
浮力 向上速度越來越快
越強對流 越窄

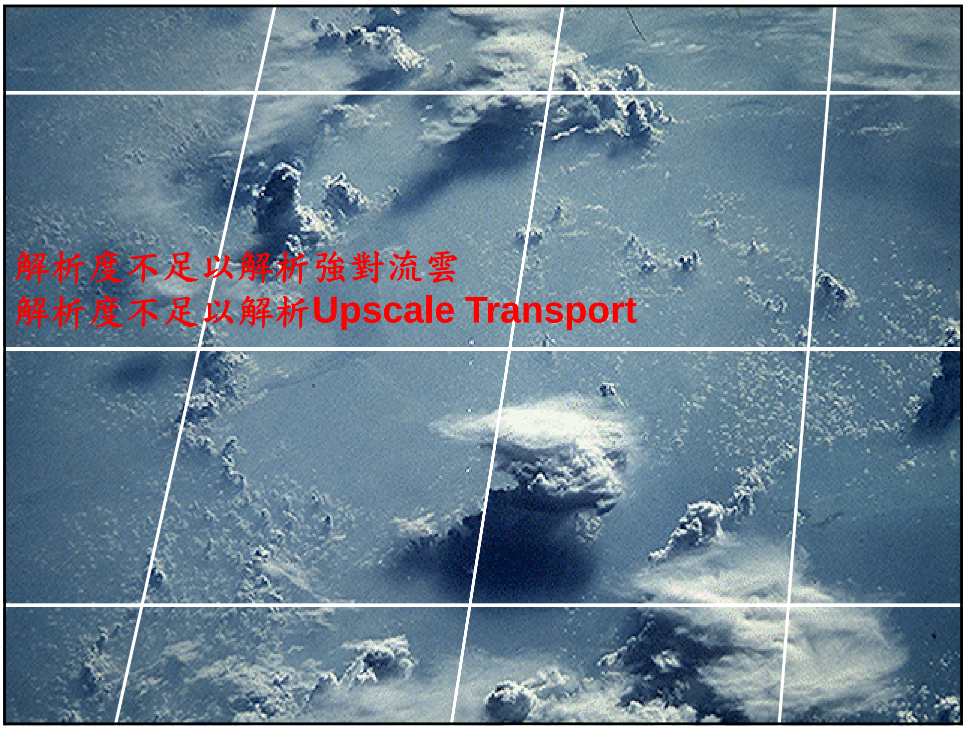
解析度不足以解析強對流雲
解析度不足以解析Upscale Transport

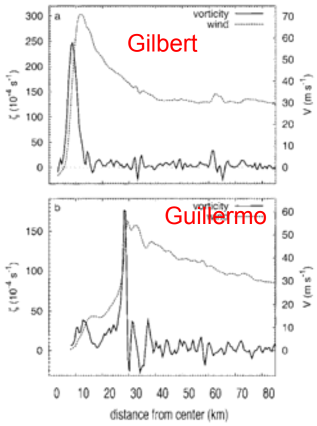

Kossin and Schubert (2001)

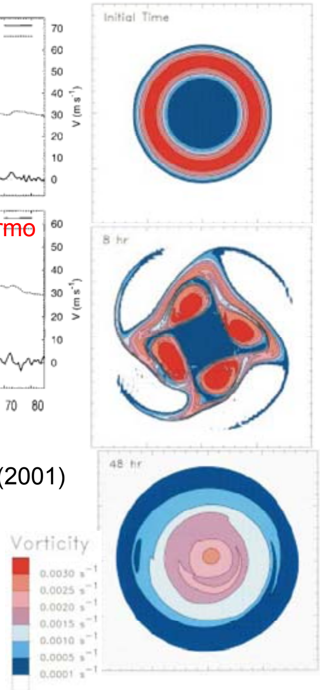

Schubert et al. (1999)

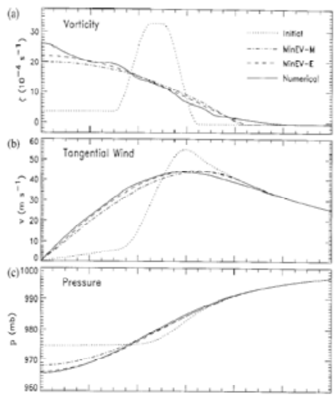

Vorticity mixing leads to Rapid Intensification !

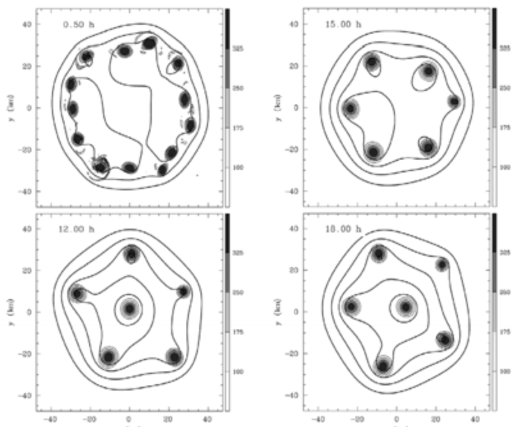

FIG. 2. Evolution of vorticity (shaded) and streamfunction contours (bold) for the numerical experiment of Kossin and Schubert (2001). Values along the label bar are in units of 10^{-4} s^{-1}. The shape of the streamlines transitions from a pentagon to a hexagon and back to a pentagon over 6 h.

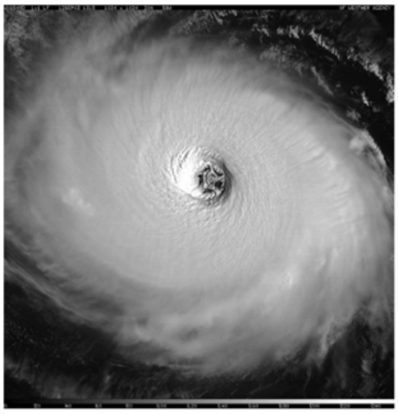

FIG. 1. Defense Meteorological Satellite Program (DMSP) image of Hurricane Isabel at 1315 UTC 12 Sep 2003. The starfish pattern is caused by the presence of six mesovortices in the eye—one at the eye center and five surrounding it.

MESOVORTICES IN HURRICANE ISABEL

BY JAMES P. KOSSIN AND WAYNE H. SCHUBERT

Importance of Asymmetric Vorticity Dynamics

A case where MPI theory failed! (Montgomery 2006)

熱力學 + 流體力學

Euler 1755

$$\frac{d}{dt}\int_{v_m} \rho\vec{v}\,dv = -\int_{\partial v_m} p\,d\vec{s}$$

$$\int_{v_m} \rho\frac{d\vec{v}}{dt}\,dv = -\int_{v_m} \nabla p\,dv$$

$$\rho\frac{d\vec{v}}{dt} = -\nabla p$$

Lagrange 1781

$$\frac{\partial\vec{u}}{\partial t} + \vec{\zeta}\times\vec{u} = -\frac{1}{\rho}\nabla p - \nabla K - \nabla\Phi$$

Rotation， Vortex

電磁學

Lorentz Force Law

$$\mathbf{F} = q(\mathbf{E} + \mathbf{v}\times\mathbf{B})$$

$$\mathbf{F} = q(-\nabla V + \mathbf{v}\times\mathbf{B})$$

Vortex cannot terminated in the fluid interior.

Helmholtz 1858

$$\frac{\partial\vec{\zeta}}{\partial t} + \vec{v}\cdot\nabla\vec{\zeta} + \vec{\zeta}\,\nabla\cdot\vec{v} = \vec{\zeta}\cdot\nabla\vec{v} + \vec{B}$$

$$\vec{B} = \nabla\times(-\frac{1}{\rho}\nabla p)$$

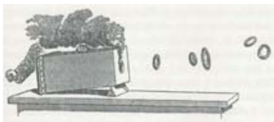

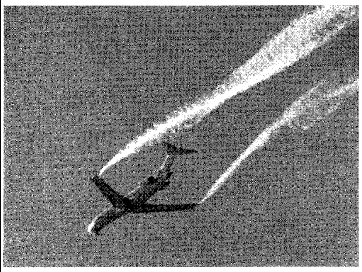

Wake Turbulence

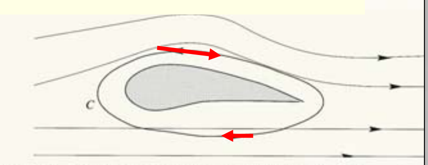

Fig. 8.10. Sketch of the flow along an airfoil. The wing is shown in g
contour C is shown by the thick solid line.

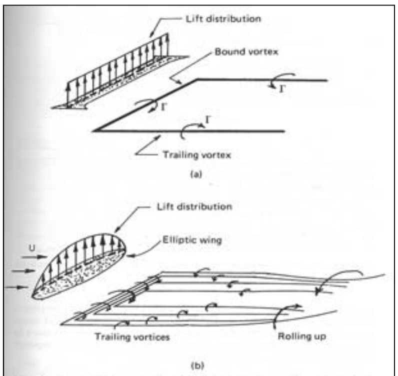

FIGURE 3.10:2 (a) A horse-shoe vortex representing a wing with a uniform lift distribution. (b) Lift distribution on an elliptic wing.

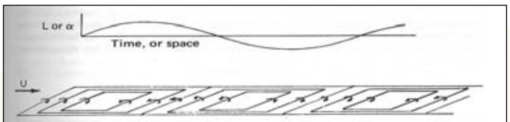

FIGURE 3.10:4 The vortices in the wake of an oscillating wing, idealized under the assumption that the lift fluctuation is very small so that the distortion of the wake due to the vortices in it is also very small. L is the lift, α is the angle of attack.

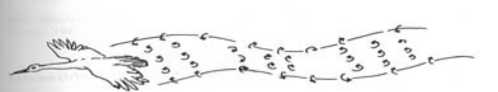

FIGURE 3.10:5 The vortex wake behind a stork in level flight.

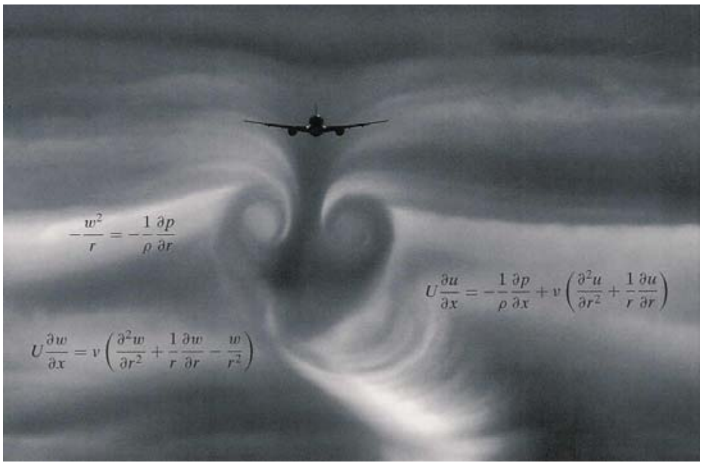

A British Airways Boeing 777-200 aircraft is approaching to land at Gatwick Airport traveling at 170 kts at approximately 1800 ft. The cloud base Is 2200 ft, RH = 83%, T = 16.8, Td = 14.5, p = 1022.2 hPa, wind = 6.4 km/h.

Jean Leon Foucault 1851

$$\frac{d^2\mathbf{x}}{dt^2} = \mathbf{g} + \frac{\mathbf{T}}{m} - 2\mathbf{\Omega} \times \frac{d\mathbf{x}}{dt}$$

$$\frac{D\mathbf{V}}{Dt} = -\frac{1}{\rho}\nabla p - 2\mathbf{\Omega} \times \mathbf{V} + \mathbf{g} + \nu\nabla^2\mathbf{V}$$

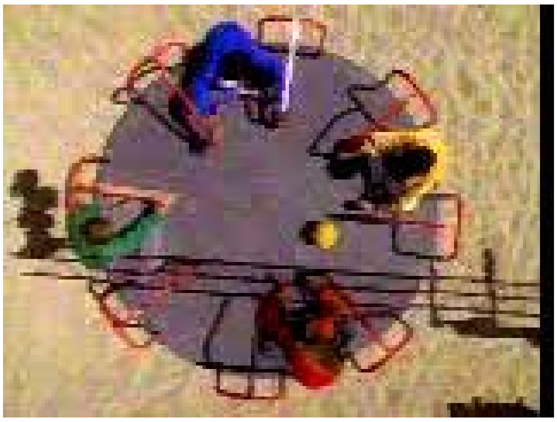

Coriolis Force

Non-inertial Frame

3D

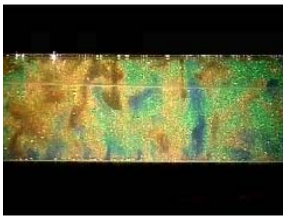

2D (strong rotation)

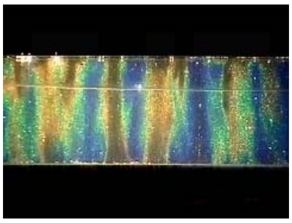

Taylor columns Vortex Tubes

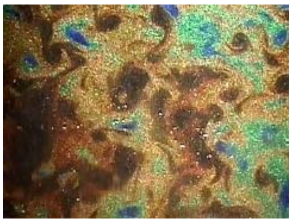

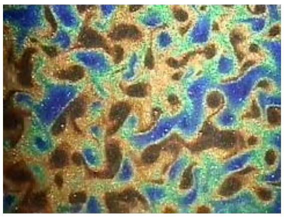

Vortices with sharp edge

Kyoto Univ. GFD group

Waves with zero potential vorticity

Non-rotation

rotation

rotation

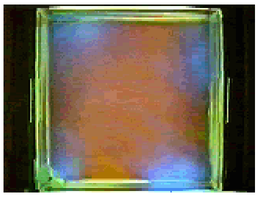

Gravity waves

Kelvin Waves
Edge waves

20th Century

Geophysical Fluid Dynamics (GFD) 地物流力
Atmospheric Oceanic Fluid Dynamics (AOFD)
is for those interested in doing research in the physics, chemistry, and/or biology of Earth fluid environment.

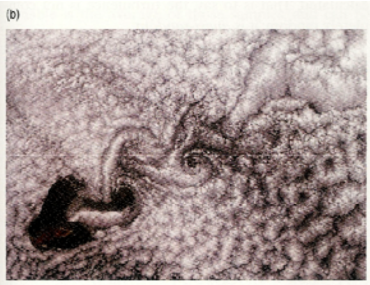

Fig. 9.2 Karman vortex streets in (a) the laboratory, for water flowing past a cylinder [From M. Van Dyke, *An Album of Fluid Motion*, Parabolic Press, Stanford, Calif. (1982) p. 56.], and (b) in the atmosphere, for a cumulus-topped boundary layer flowing past an island [NASA MODIS imagery].

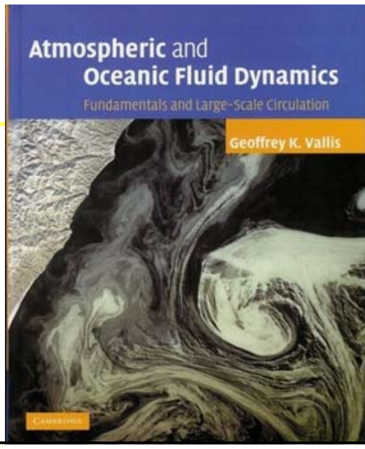

2D Turbulence

Stratification and/or Rotation
Vortex Waves Turbulence

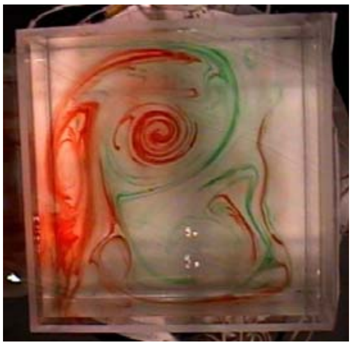

$$\frac{\partial \zeta}{\partial t} + u\frac{\partial \zeta}{\partial x} + v\frac{\partial \zeta}{\partial y} = \nu \nabla^2 \zeta$$

$$u = -\frac{\partial \psi}{\partial y}, \qquad v = \frac{\partial \psi}{\partial x}.$$

$$\frac{\partial \zeta}{\partial t} + \frac{\partial(\psi, \zeta)}{\partial(x, y)} = \nu \nabla^2 \zeta$$

Ocean Spice

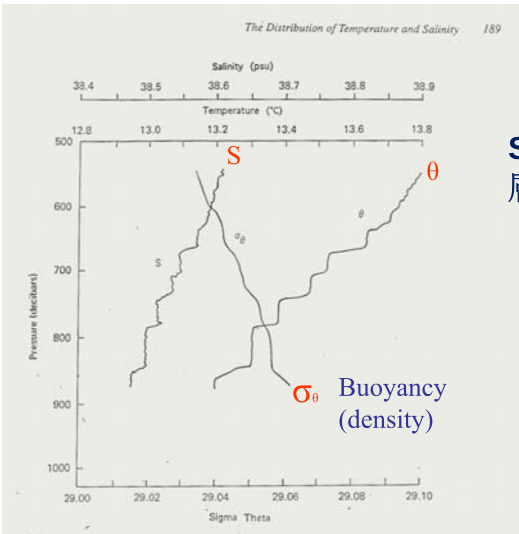

Stratification
層化

Figure 8.19 Temperature steps are usually concurrent with steps in the salinity gradient. The two tend to offset one another so that the density gradient is relatively smooth. (After Molcard and Williams, *Me. Soc. Roy. des Sci. de Leige*, 7, 1975.)

Some of the horizontal layering implied by discontinuities such as in Figure 8.19 can be explained on the basis of *stirring* (see "stirring and mixing" in Chapter 4). Because stirring in the horizontal plane is several orders of magnitude larger than that in the vertical, as different types of water mix horizontally, sharp vertical gradients can be expected to occur occasionally. A variety of additional mechanisms have been suggested for generating such fine structure, including turbulence generated by both bottom topography and surface waves as well as the breaking of small-scale internal waves (Figure 8.20).

Multiple Scale Interactions in Vortex

Wave mean flow interaction in stable stratified fluid
Turbulent feed back to the vortex mean flow

2D turbulence

Kyoto Univ. GFD group

$$\frac{d}{dt}\int E(k)dk = 0. \qquad \frac{d}{dt}\left(\int k^2 E(k)dk\right) = \frac{d}{dt}\int Z(k)dk = 0,$$

$$\frac{d}{dt}\left(\int (k-k_1)^2 E(k)dk\right) > 0$$

$$\frac{d}{dt}\left(\int k^2 E(k)dk + k_1^2\int E(k)dk - 2k_1\int kE(k)dk\right) > 0$$

$$\frac{d}{dt}\left(\frac{\int kE(k)dk}{\int E(k)dk}\right) < 0,$$

Kinetic energy moves toward large scales

$$\frac{d}{dt}\left(\int (k^2-k_1^2)^2 E(k)dk\right) > 0$$

$$\frac{d}{dt}\left(\int k^2 Z(k)dk + k_1^4\int E(k)dk - 2k_1^2\int k^2 E(k)dk\right) > 0$$

$$\frac{d}{dt}\left(\frac{\int k^2 Z(k)dk}{\int Z(k)dk}\right) > 0,$$

Enstrophy moves toward small scales

Non-divergent barotropic model (Nearly Inviscid Fluid)

$$\frac{\partial}{\partial t}\zeta + J(\psi, \zeta) = \upsilon \nabla^2 \zeta \qquad \nabla^2 \psi = \zeta$$

The energy and enstrophy relations

$$\frac{d\mathcal{E}}{dt} = -2\,\upsilon\,\mathcal{Z}$$

$$\frac{d\mathcal{Z}}{dt} = -2\,\upsilon\,\mathcal{P}$$

$$\mathcal{E} = \iint \frac{1}{2}\left(u^2 + v^2\right) dx\,dy$$ kinetic energy

$$\mathcal{Z} = \iint \frac{1}{2}\zeta^2\,dx\,dy$$ enstrophy

$$\mathcal{P} = \iint \frac{1}{2}\nabla\zeta \cdot \nabla\zeta\,dx\,dy$$ palinstrophy

Batchelor 1969

$E \sim p'^2 / L^2$ (KE) geostrophy

$Z \sim p'^2 / L^4$ (Enstrophy)

KE nearly conserved $L \sim p'$

Enstrophy cascade L↑ (L increase Z decrease)

Selective Decay of 2D turbulence

The vortices become, on the average, larger, stronger, and fewer.

Merger and Axisymmetrization Dynamics

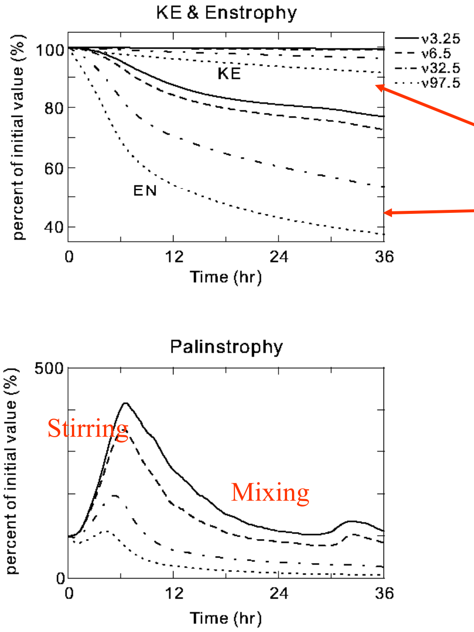

KE nearly conserved

Enstrophy cascade

Selective Decay of 2D turbulence

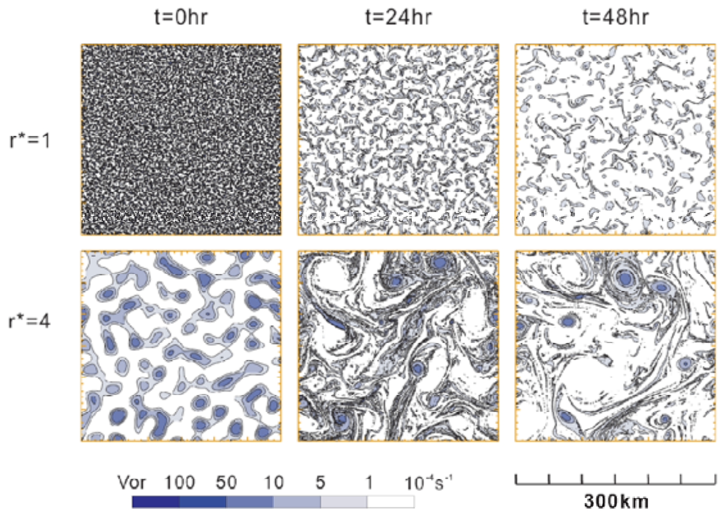

Fewer and stronger vortices !!!

小尺度變大尺度
Upscale transfer

Coherent structure with filamentations in 2-D turbulence

Weiss(1981,1991), Rozoff et al. (2004)

$$\frac{D}{Dt}(\nabla\zeta) = -J(\nabla\psi,\zeta)$$

$$\rightarrow \nabla\zeta(t) \propto \exp(\lambda t) \quad \lambda = \pm\frac{1}{2}\sqrt{Q} = \pm\frac{1}{2}\sqrt{S_1^{\,2} + S_2^{\,2} - \zeta^2}$$

$$S_1 = \frac{\partial u}{\partial x} - \frac{\partial v}{\partial y} \quad \text{(stretch deformation)}$$

$$S_2 = \frac{\partial v}{\partial x} + \frac{\partial u}{\partial y} \quad \text{(shear deformation)}$$

Q > 0 (strain dominates)
→vorticity gradient will be stretched
Q < 0 (vorticity dominates)
→vortex is stable (survival of eyewall meso-vortices)

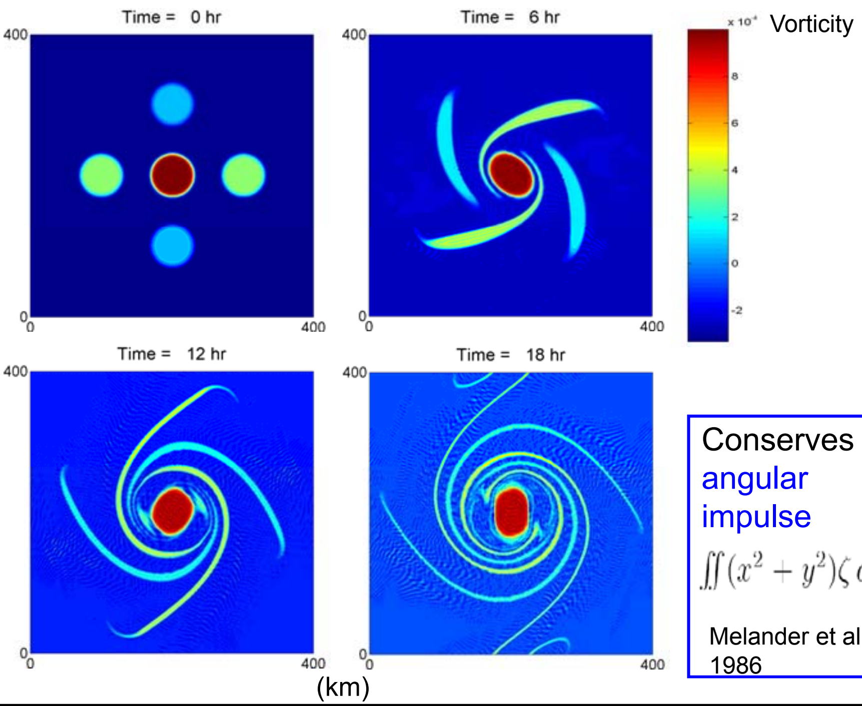

Conserves the angular impulse

$$\iint (x^2+y^2)\zeta \, dx dy$$

Melander et al. 1986

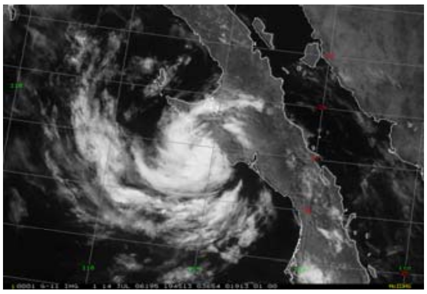

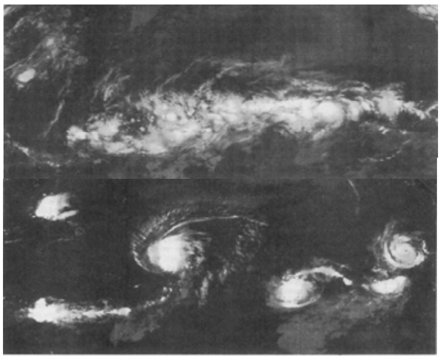

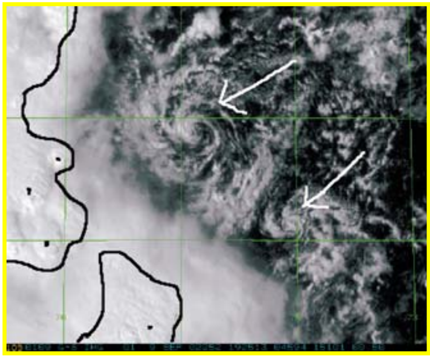

賀伯颱風的橢圓形眼　Kuo et al. 1999 JAS

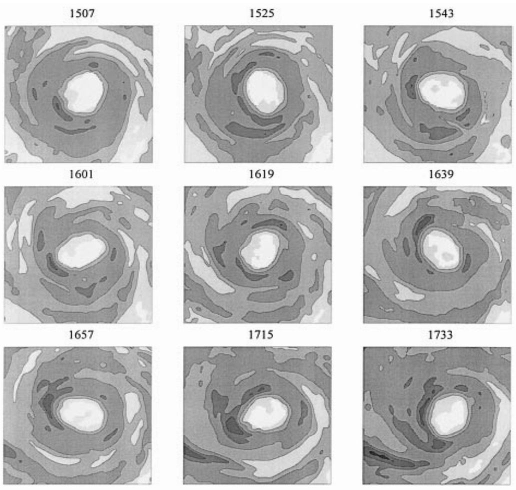

FIG. 1. Horizontal distribution of maximum reflectivity in the vertical column for Typhoon Herb from the Central Weather Bureau WSR-88D (10 cm) radar at Wu-Feng Mountain on 31 Jul 1996. The sequence of images is from left to right and from top to bottom. The time interval between each image is approximately 18 min. The local time of observation is indicated on top of each image. The major axis radius in the eye region is about 30 km and the minor axis radius is about 20 km. The nine images illustrate one eye rotation period of 144 min.

144 min rotation period

Lamb, 1932

Kirchhoff vortex （nonlinear）

$$\zeta \frac{ab}{(a+b)^2} = \omega$$

rotating period **P** = $\dfrac{2\pi}{\zeta}\dfrac{(a+b)^2}{ab}$

Kelvin PV wave （linear）

$$c = V_{max}\left(1-\frac{1}{m}\right) \qquad m=2$$

$$\sim \frac{2\pi}{\omega} = \frac{2\pi}{2\dfrac{V_{max}}{r}} * 4 = \frac{2\pi}{\zeta} * 4$$

Vortex Rossby Waves

Deep convections rotation 144 min

Eye rotation is nonlinear

$J(\psi,\zeta) \quad >> \quad J(\psi,\zeta)$

EXP 1 EXP 2

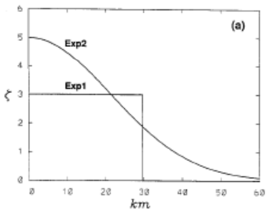

$$\frac{\partial}{\partial t}\zeta + J(\psi,\zeta) = 0$$

T= 0 min

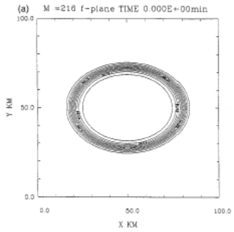

T= 0 min

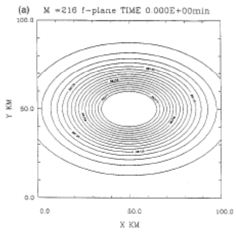

T= 144 min

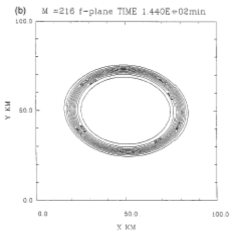

T= 144 min

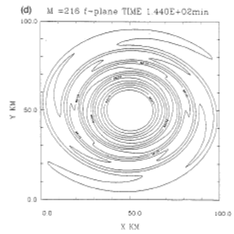

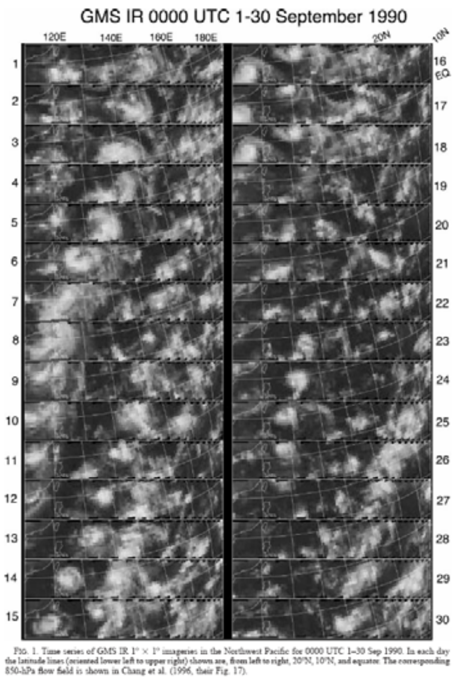

Kuo et al.(2001)

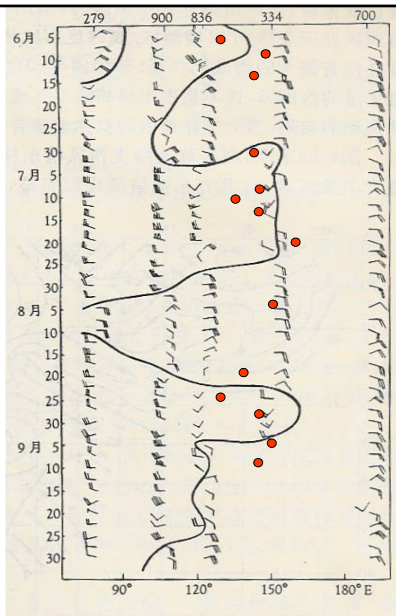

图3 1958年6～9月印度南端到太平洋赤道附近700 hPa 东西风分界线与台风发生的关系

謝與陳(1963)

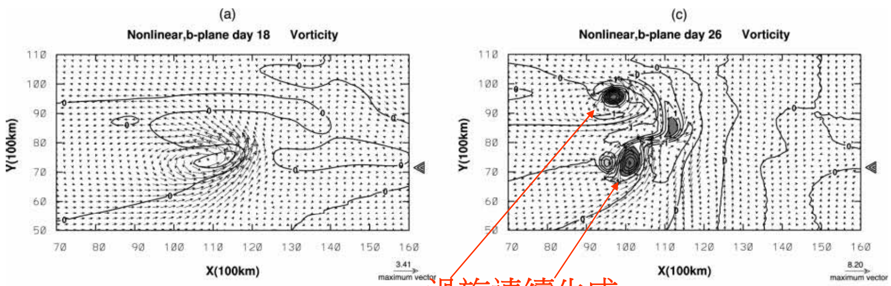

Beta Rossby number (V/ β r ^2) ~ 1

渦旋連續生成

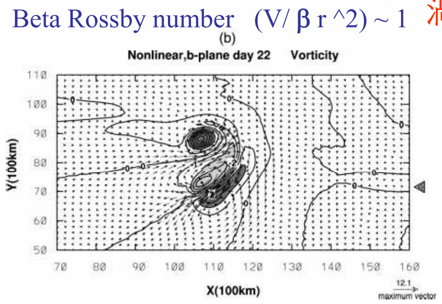

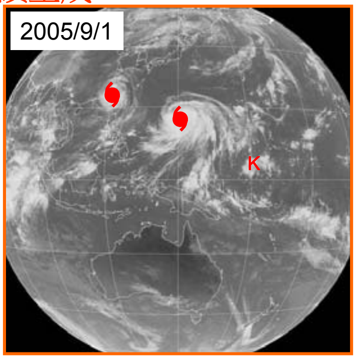

FIG. 11. Same as in Fig. 10 except for the nonlinear β-plane

Kuo et al. 2001

Bowmen and Mangus (1993)

Observations of deformation and mixing of the total ozone field in the Antarctic polar vortex

Surf Zone Dynamics

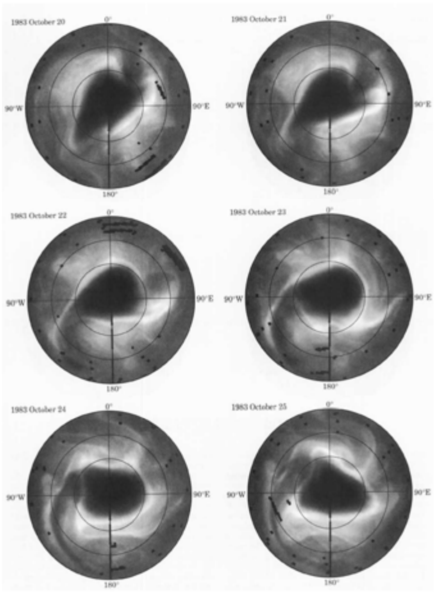

Fig.1: Daily TOMS images of total ozone in the Southern Hemisphere for six consecutive days in October 1983. Latitude circles are drawn at 40˚,60˚, and 80 ˚S. The outermost latitude is 20 ˚S.

Huang and Robinson 1998

Forcing added

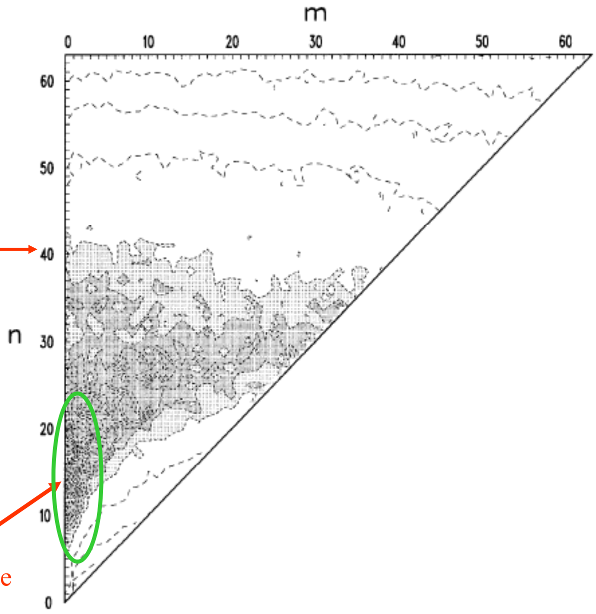

Inverse energy cascade to zonal Harmonics

FIG. 2. Energy spectrum $E(m, n)$ of an ensemble mean at day 80 of 10 decaying turbulence experiments. The magnitude of the spectrum is normalized by the maximum value on the map. Contour levels are 0.0001, 0.001, 0.01, 0.1–0.9 with increment 0.1. Area with $E(m, n) > 0.1$ is lightly shaded, $E(m, n) > 0.2$ heavily shaded.

Jupiter

Rotational period 9.84hr

The Great Red Spot

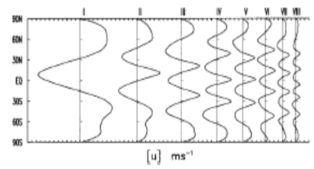

Huang and Robinson 1998

abscissa represents 1 m s^{-1}.

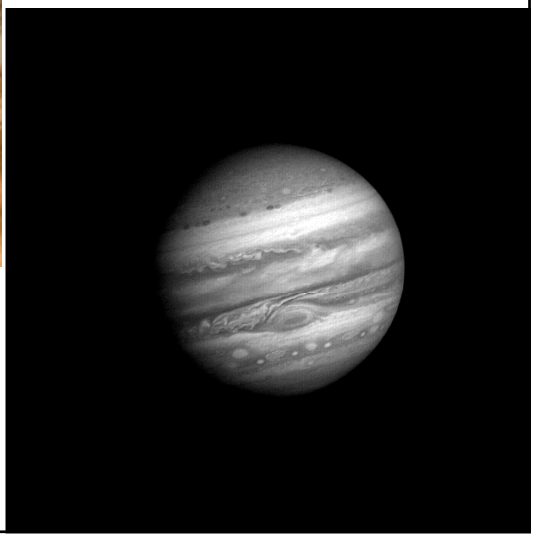

Electron density redistribution in experimental plasma physics

single sign charge
+
axial magnetic field
confinement

$$E = -\nabla\psi$$

$$\nabla \cdot E = -\nabla^2\psi = \frac{\rho}{\epsilon}$$

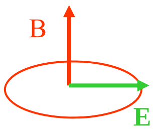

$\vec{E}\times\vec{B}$ drift

Coriolis force

Axisymmetrization 軸對稱化

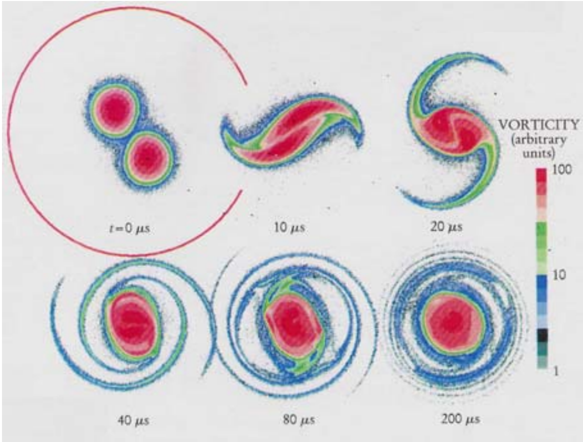

Core is protected, thin filaments from edges

Binary vortex interaction

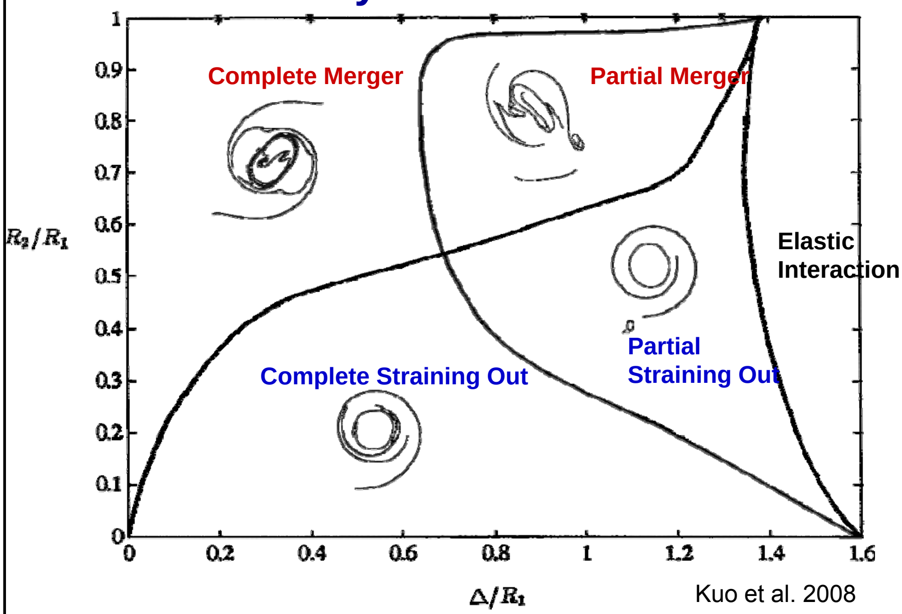

Kuo et al. 2008

(Adapted from Dritschel and Waugh 1992.)

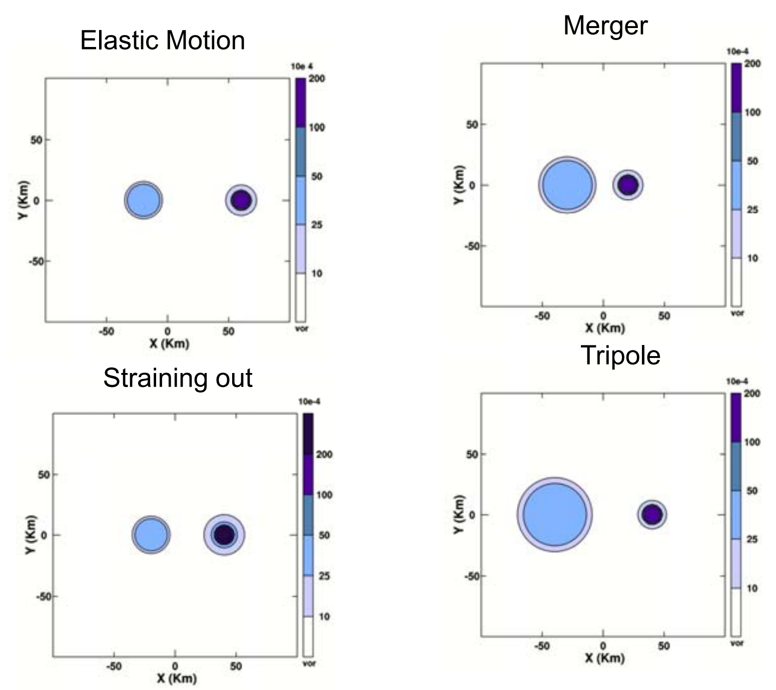

雙颱風互繞（藤原效應）合併 ---- 颱風 PAT 與 RUTH

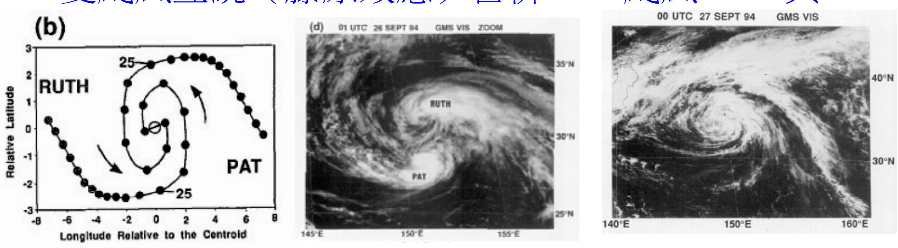

中尺度對流系統互繞

Simpson et al. 1998

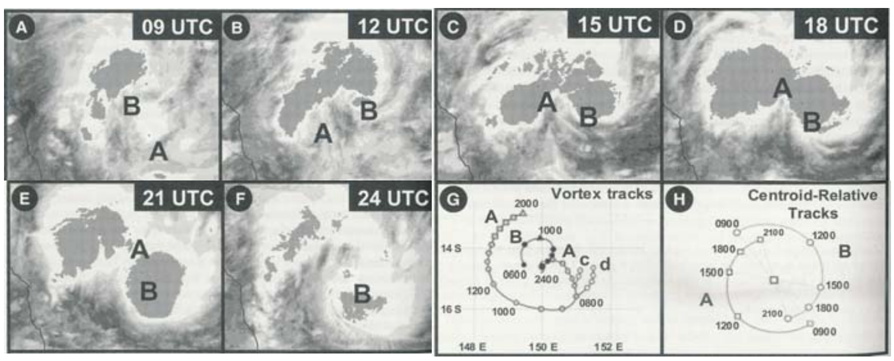

納莉颱風眼附近的中尺度渦旋

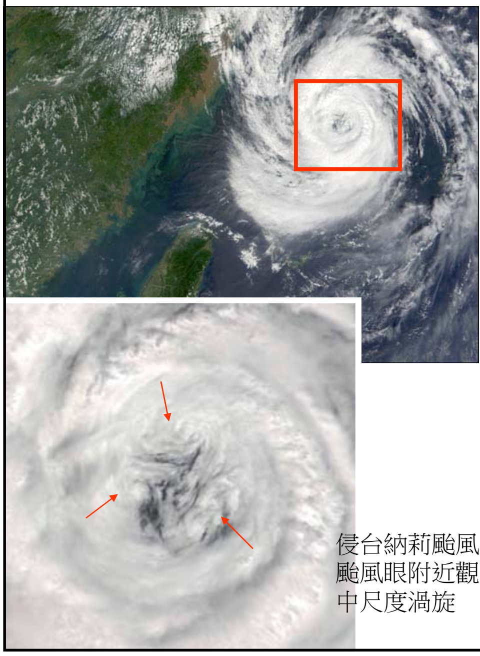

侵台納莉颱風登陸前
颱風眼附近觀測到3 個
中尺度渦旋

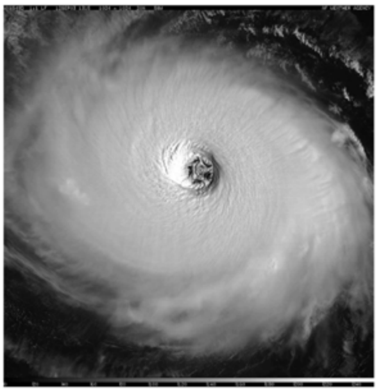

Fig. 1. Defense Meteorological Satellite Program (DMSP) image of Hurricane Isabel at 1315 UTC 12 Sep 2003. The starfish pattern is caused by the presence of six mesovortices in the eye—one at the eye center and five surrounding it.

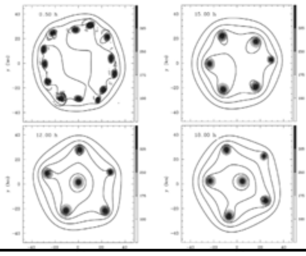

颱風渦旋合併動力探討研究

Kuo, H.-C., G. T.-J. Chen, and C.-H. Lin, 2000: Merging processes of tropical cyclone Zeb and Alex. *Mon. Wea. Rev.*, **128**, 2967-2975.

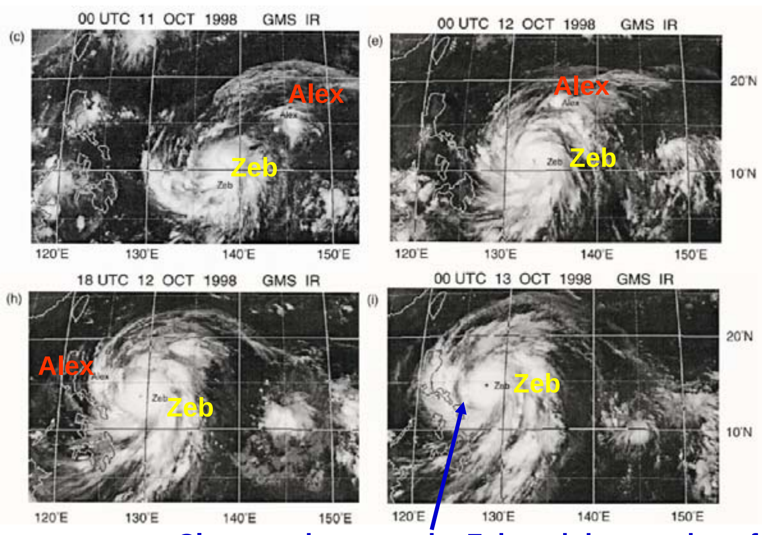

Clear gap between the Zeb and the remains of Alex

Concentric eyewalls near Taiwan

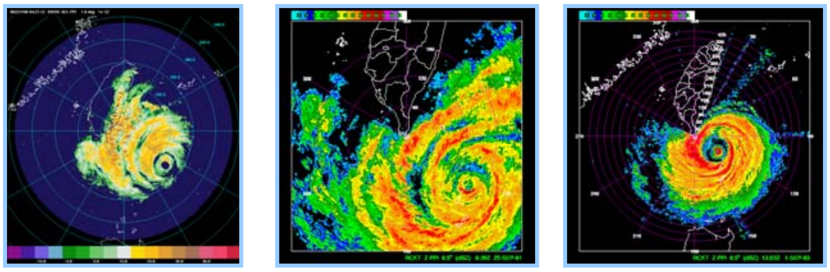

Bilis(2000) Lekima(2001) Dujuan(2003)

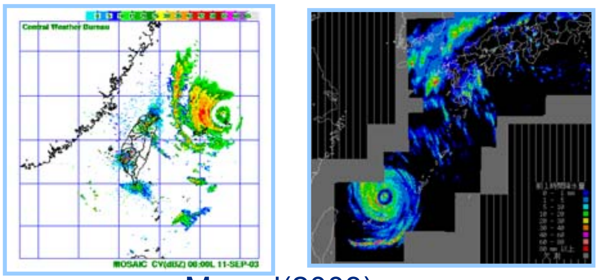

Maemi(2003)

WNPAC Concentric eyewalls formation locations, intensity, and tracks

Kuo et al. (2009)

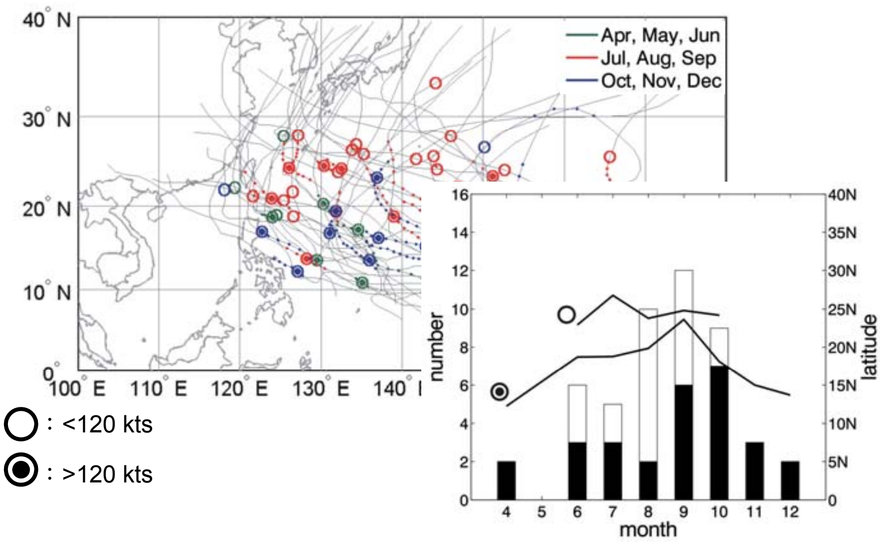

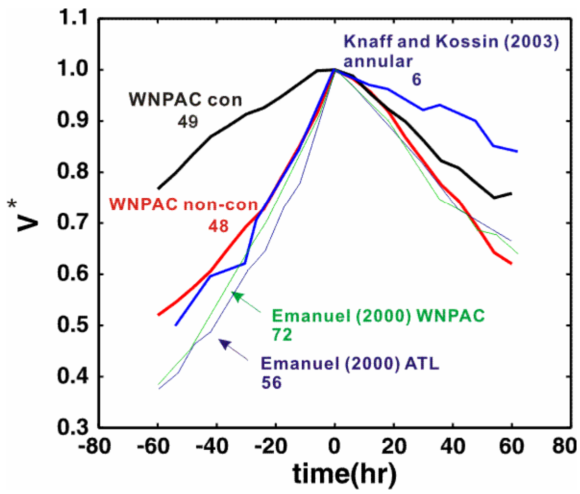

Key feature of concentric eyewall formation appears to the maintenance of a relative high intensity for a longer duration prior to formation, rather than a rapid intensification process that can reach a high intensity.

Kuo et al. 2009

Knaff and Kossin (2003)

- color-enhanced IR image of Hurricane Luis (1995) at 2015 UTC 3 Sep

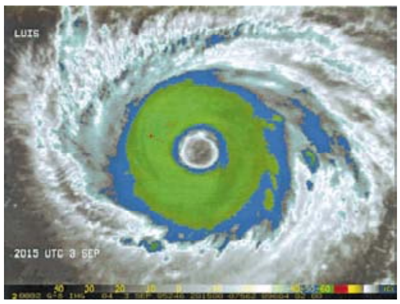

dimensionless	24-h weakening
ATL(56)	0.14
Annular hurricanes(6)	0.05

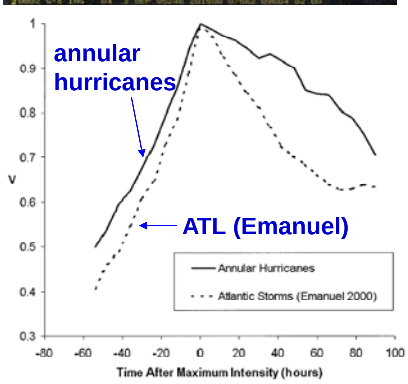

A major issue in understanding changes in typhoon intensity

Black and Willoughby (1992)
Hurricane Gilbert (1988)

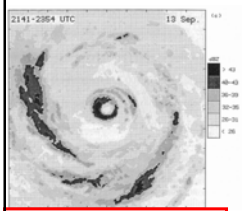

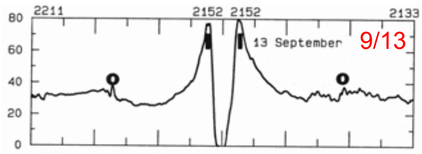

Development of symmetric structure from asymmetric convection in 12 hours

The contraction of the Outer tangential wind maximum

Core vortex intensity remains approximately the same during the contraction period

Inner core dissipate, TC weakens

Black and Willoughby (1992)

Vertical cross sections of radar reflectivity of the concentric eyewall

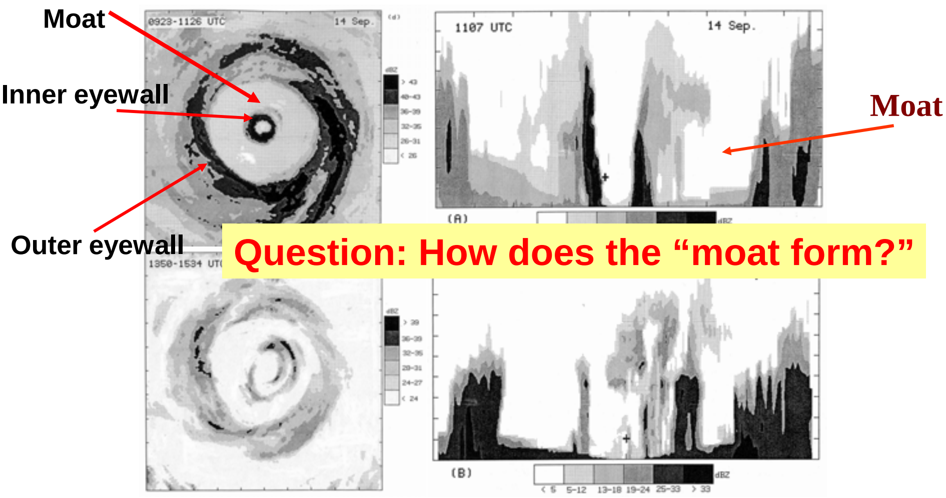

Question: How does the "moat form?"

Concentric Eyewall formation

Kuo, H.-C., L.-Y. Lin, C.-P. Chang, and R. T. Williams, 2004: The formation of concentric vorticity structure in typhoons. *J. Atmos. Sci.*, **61**, 2722-2734.
Kuo, H.-C., W. H. Schubert, C.-L. Tsai, and Y.-F. Kuo, 2008: Vortex interactions and barotropic aspects of concentric eyewall formation. *Mon.Wea. Rev.,* **136,** 5183–5198.

0935-1935 LST

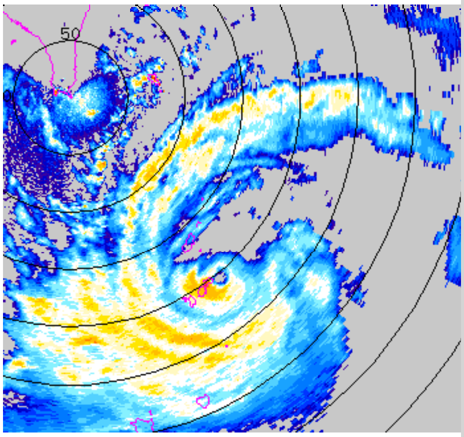

Typhoon Lekima (2001)

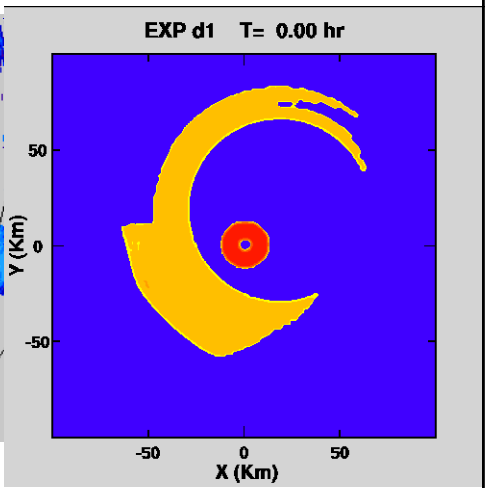

Binary vortex interaction

Kuo et al. (2004,2008)

【Variables】

$R_1, R_2; \Delta; \zeta_1, \zeta_2$ Beta-skirt

【Parameters】

- Vortex radius ratio $(r) = \frac{R_1}{R_2}$
- Dimensionless gap $(\frac{\Delta}{R_1})$
- Vortex strength ratio $(\gamma) = \frac{\zeta_1}{\zeta_2}$

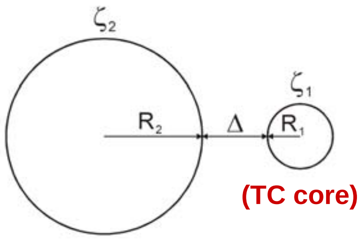

- An extension of Dritschel and Waugh's (1992) work.
- In addition to the radii ratio and the normalized distance between the two vortices, the vorticity ratio is added as a third external parameters.

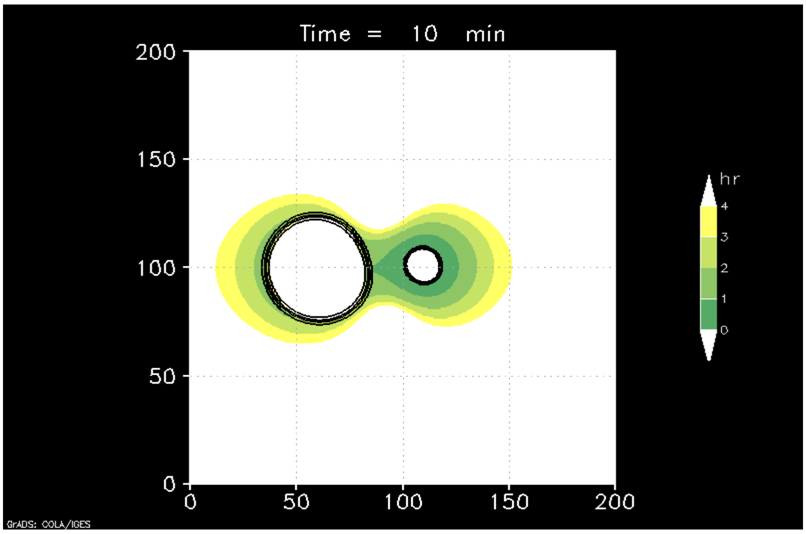

Thoughts from the 80's and 90's

Shapiro and Willoughby (1982) and Schubert and Hack (1982) proposed that heating-vorticity interaction can lead to convective-ring contraction.

$$d\zeta/dt \sim \zeta \nabla \cdot \mathbf{V}$$

Stronger ζ near the TC core favors the inward response

Symmetrical Model

Moat formation and eyewall replacement are related to the subsidence and the moisture cut-off.

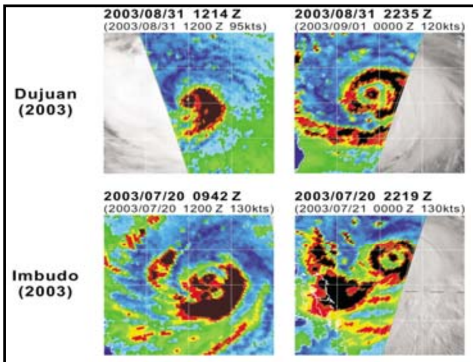

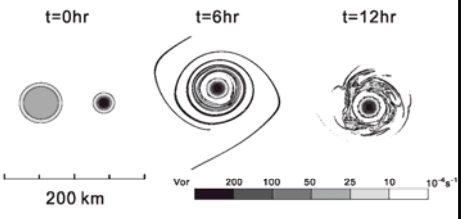

The contraction and the increase of the secondary wind maximum by nonlinear advection dynamics.

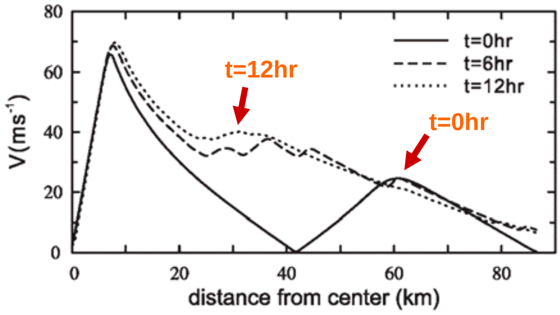

$$\gamma = \frac{\zeta_1}{\zeta_2}$$

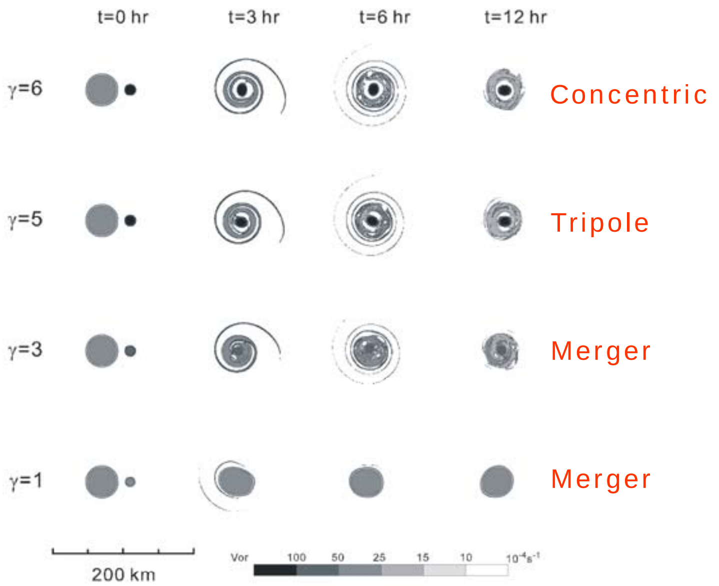

Figure 3: The sensitivity of the vorticity field in the binary vortex experiments with respect to the vorticity strength ratio (γ) at hour 0, 3, 6 and 12 with the dimensionless gap Δ/R_1=1, and the vortex radius ratio r=1/3.

$\gamma = 10$

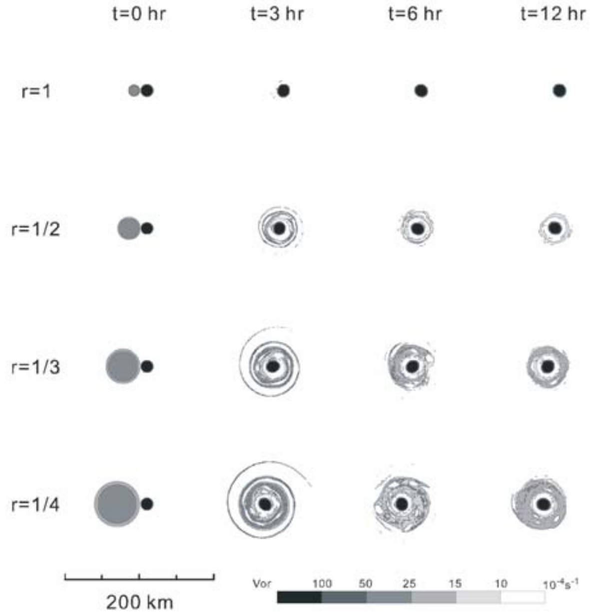

Figure 6: Similar to Figure 5 except that the dimensionless gap $\Delta/R_1=0$ and the vorticity strength ratio $\gamma=10$.

Same strain outside the RMW but different core vortex strength

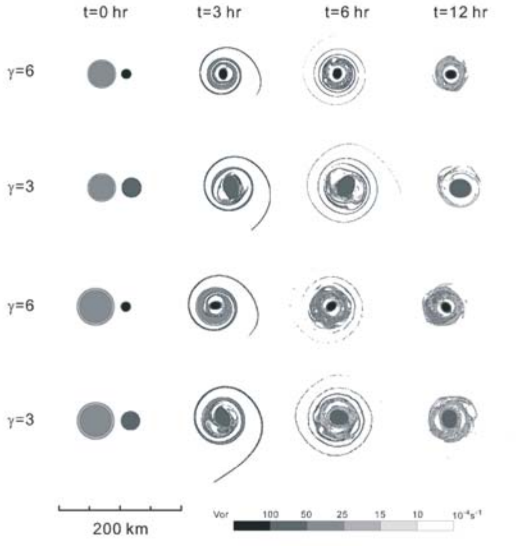

Figure 9: The sensitivity of the vorticity field in the binary vortex experiments with the core vortices process the same maximum wind but different radius of vorticity field. Two core vortices considered have the vorticity and radius of ($1.8 \times 10^{-2}s^{-1}$, 10 km) and ($0.9 \times 10^{-2}s^{-1}$, 20 km) respectively. The dimensionless gap is 1 in the experiments. The outer vortices considered have the radius of 30 km and 40 km respectively.

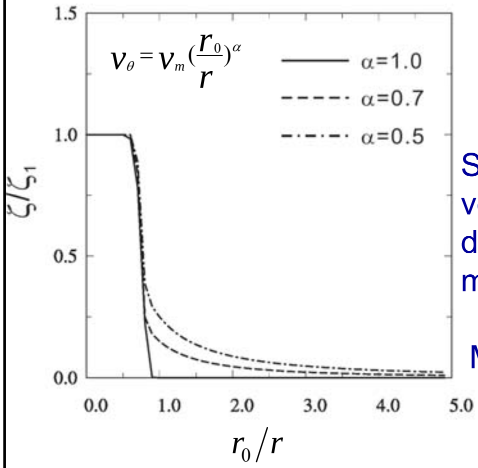

Skirt of significant cyclonic relative vorticity (slow tangential wind decrease outside the radius of maximum wind).

Mallen et al. 2005

Radial profile of the vorticity for the core vortex with the skirt parameter (α) 1.0, 0.7 and 0.5.

Double eyewall of different sizes maybe explained by the binary vortex interaction with skirted parameter

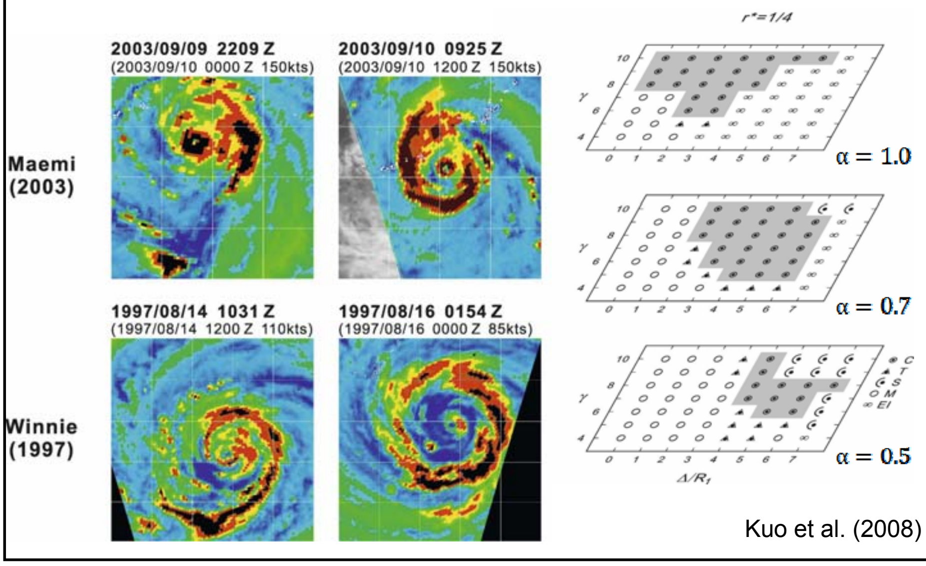

Kuo et al. (2008)

D12112 TERWEY AND MONTGOMERY: MODELED SECONDARY EYEWALL FORMATION D12112

JGR 2008

Table 1. List of Secondary Eyewall Formation Hypotheses With Summary of Relevance to our Modeled Hurricanes[a]

Authors	Hypothesis Summary	Relevance to Current Model Results	Type
Willoughby et al. [1982] borrowing from the squall line research of *Zipser* [1977]	Downdrafts from the primary eyewall force a ring of convective updrafts.	Few downdraft-forced updrafts during this time in the simulations.	O
Willoughby [1979]	Internal resonance between local inertia period and asymmetric friction due to storm motion.	No systematic storm motion in the simulated storms.	A
Hawkins [1983]	Topographic effects	No topographic forcing in the simulations.	O
Willoughby et al. [1984]	Ice microphysics	"Warm-rain" (no-ice) sensitivity case also produces secondary eyewall.	A
Molinari and Skubis [1985] and *Molinari and Vallaro* [1989]	Synoptic-scale forcings (e.g., inflow surges, upper-level momentum fluxes)	No synoptic-scale forcings in the simulations	O
Montgomery and Kallenbach [1997], *Camp and Montgomery* [2001] and *Terwey and Montgomery* [2003]	Internal dynamics-axisymmetrization via sheared vortex Rossby wave processes; collection of wave energy near stagnation or critical radii	Possible explanation	N
Nong and Emanuel [2003]	Sustained eddy momentum fluxes and WISHE feedback	Possible explanation	A
Kuo et al. [2004, 2008]	Axisymmetrization of positive vorticity perturbations around a strong and tight core of vorticity.	Possible explanation	N

[a]The type column refers to the type of model or observations that were used to formulate the hypothesis. O stands for observationally-based; A stands for axisymmetric model; N stands for nonaxisymmetric model.

Kuo et al. 2008

D12112 TERWEY AND MONTGOMERY: MODELED SECONDARY EYEWALL FORMATION D12112

JGR 2008

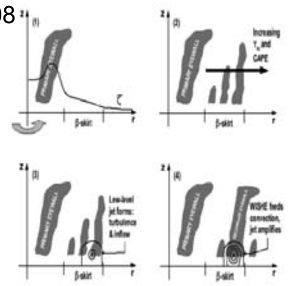

Figure 6. Proposed conceptual model of the β-skirt axisymmetrization (BSA) mechanism for the formation of a secondary eyewall.

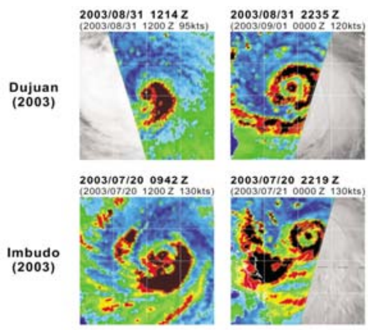

Importance of the vorticity axisymmetrization dynamics + convections.

Need to understand both the vorticity generating meso-scale processes in the TC environment and the detail core structure.

Summary

Tropical cyclones of sufficient strength ($\geq$ 120 kts) often form double eyewalls. Inner eyewall weakens and/or die.

Area of asymmetric convection outside the core vortex that wraps around the inner eyewall to form the concentric eyewalls in about 12 hours.

The contraction of the secondary wind maximum and the formation of the moat are features of the vorticity dynamics. The moat formation by subsidence, rapid filamentation, and advective dynamics.

Double eyewall of different sizes maybe explained by the binary vortex interaction with skirted parameter.

The pivotal role of the vorticity strength of the core vortex in maintaining itself, and in strectching, organizing and stabilizing the outer vorticity field, and the shielding effect of the moat to prevent further merger and enstrophy cascade processes in concentric eyewall dynamics.

Vorticity generation in the core and in the environment (via mesoscale convections) are of great importance!

Large variability in vertical motion.

High resolution appears to be crucial in concentric eyewall simulation.

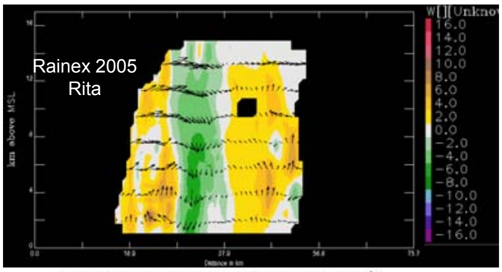

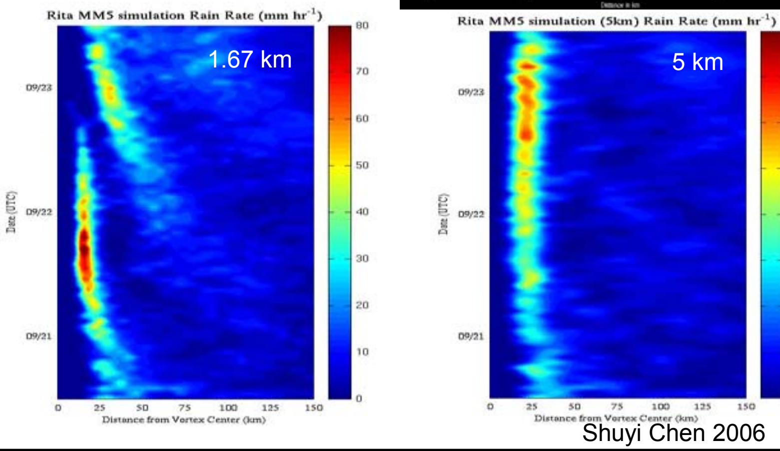

Shuyi Chen 2006

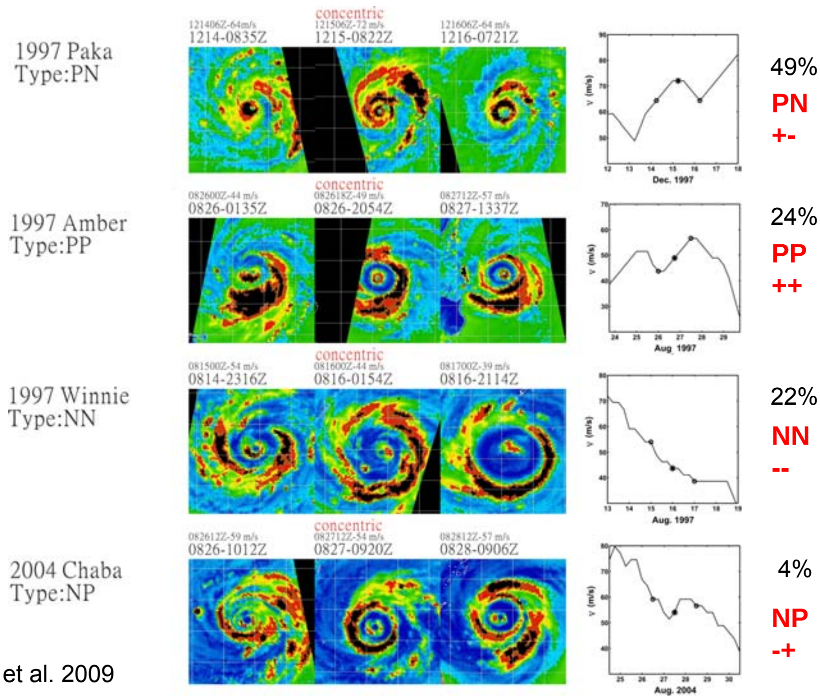

Kuo et al. 2009

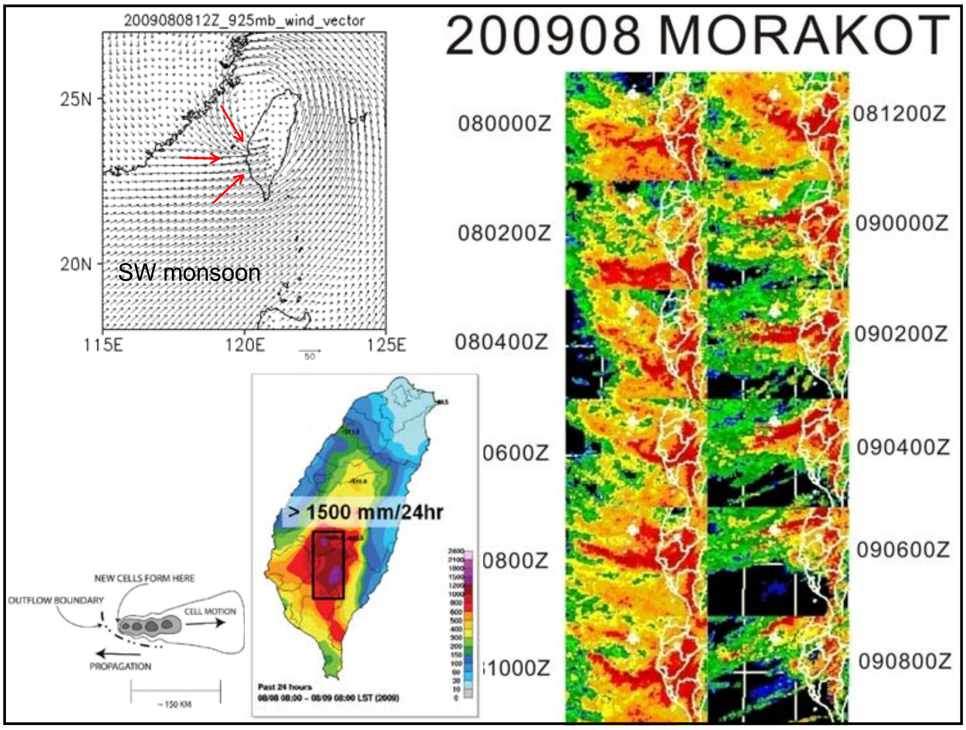

一杯咖啡，古今往事盡付笑談中。

The best part of waking up, is the vortex in your cup!

$$\frac{D\theta}{Dt}=\frac{\partial\theta}{\partial t}+\vec{V}\cdot\nabla\theta=\nu\nabla^2\theta$$

$$C=\frac{1}{2}\int\nabla\theta\cdot\nabla\theta\;dV$$

$$\frac{dC}{dt}=\int(\vec{V}\cdot\nabla\theta)\nabla^2\theta\;dV-\nu\int(\nabla^2\theta)\,dV$$

Stirring **Mixing**

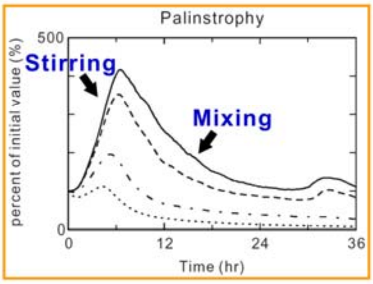

Coffee with white

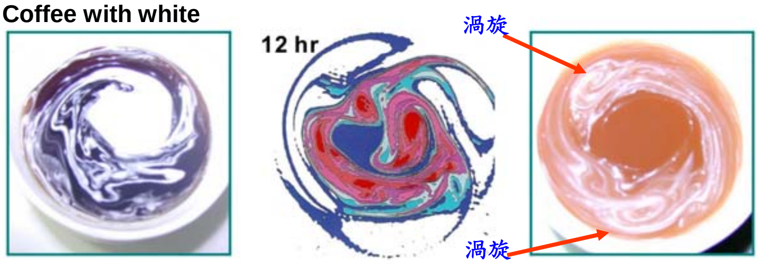

Thank you!

A painting with vortices and filaments!

1997-2006
62 CE cases

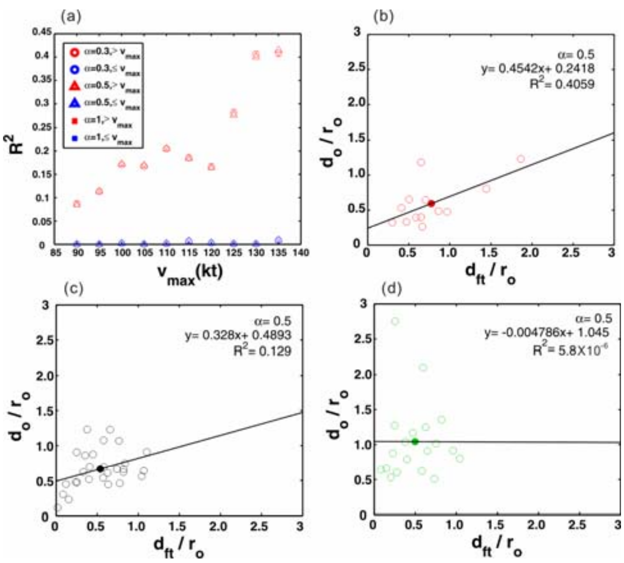

Cat 5

Cat 4

else

The rapid filamentation process tends to make an important contribution to the organization of the moat in strong typhoons, especially in cases where the maximum winds are greater than 130 kts.

Kuo et al. (Nov. 2009 MWR)

Filamentation time (Rozoff et al.,2006)

$$\frac{D}{Dt}(\nabla\zeta) = -J(\nabla\psi, \zeta)$$

$\frac{1}{2}S_1 = u_x - v_y$, stretching deformation

$\frac{1}{2}S_2 = v_x + u_y$, shearing deformation

(i) when $S_1^2 + S_2^2 - \zeta^2 < 0$, rotation dominated

$$\nabla\zeta(t) \propto \exp\left[\frac{1}{2} i(\zeta^2 - S_1^2 - S_2^2)^{\frac{1}{2}} t\right]$$

(ii) when $S_1^2 + S_2^2 - \zeta^2 > 0$, strain dominated

$$\nabla\zeta(t) \propto \exp\left[\frac{1}{2}(S_1^2 + S_2^2 - \zeta^2)^{\frac{1}{2}} t\right]$$

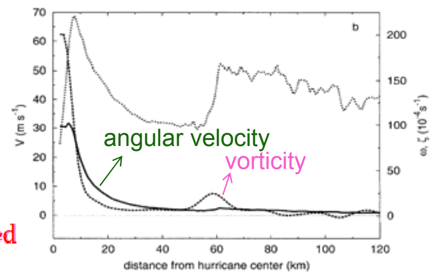

- The strong differential rotation associated with the core vortex

- $\tau_{fil} = 2(S_1^2 + S_2^2 - \zeta^2)^{-1/2} < 30\,\text{min}$: rapid filamentation time

Elastic interaction regime

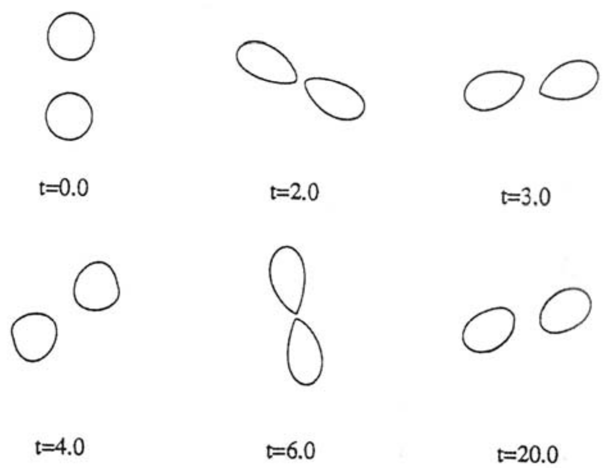

Merger regime

partial merger (PM)

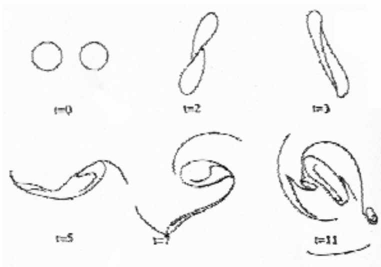

complete merger (CM)

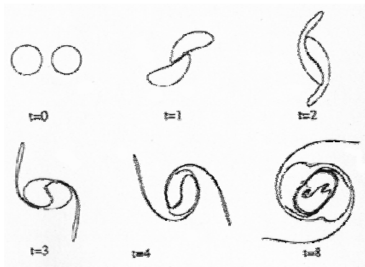

Why ‘merger’ ?

- Chang (1983) – diabatic heating
- DeMaria & Chan (1984) – vortex vorticity gradient
- Dritschel and Waugh (1992)
  – advection + selective decay of 2D turbulence

Chang (1983)

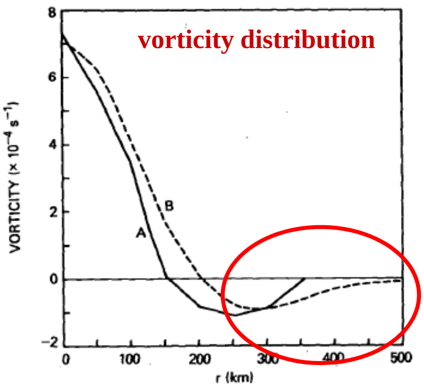

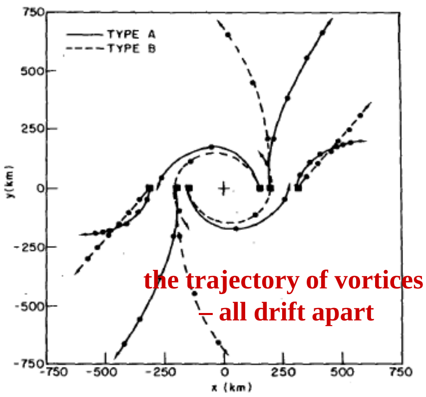

non-diabatic heating

Chang (1983)

diabatic heating

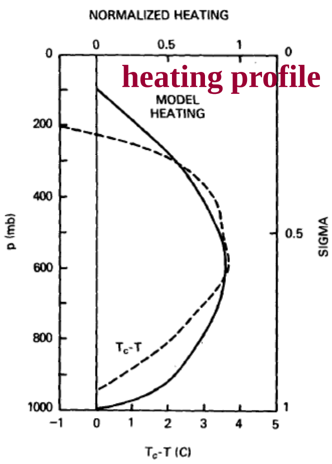

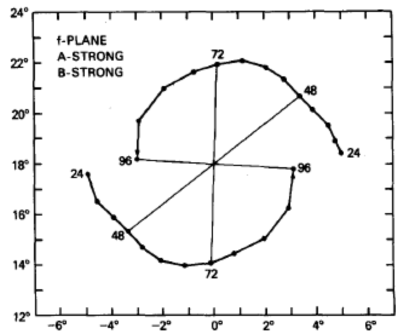

$$\frac{dQ}{dt} = 200\,(K\;day^{-1})$$

The distance between two vortices decreases with time

DeMaria & Chan (1984)

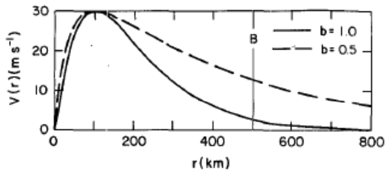

$$V(r) = V_m\left(\frac{r}{r_m}\right)\exp\left\{\frac{1}{b}\left[1-\left(\frac{r}{r_m}\right)^b\right]\right\},$$

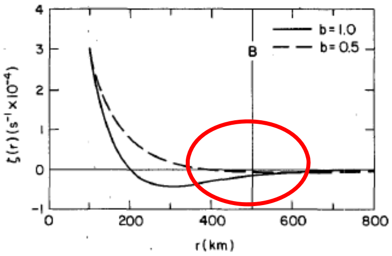

$$\zeta_{(r)} = \frac{2V_m}{r_m}\left[1-\frac{1}{2}\left(\frac{r}{r_m}\right)^b\right]\exp\left\{\frac{1}{b}\left[1-\left(\frac{r}{r_m}\right)^b\right]\right\}$$

b : the factor determines the rate of tangential wind decays

DeMaria & Chan (1984)

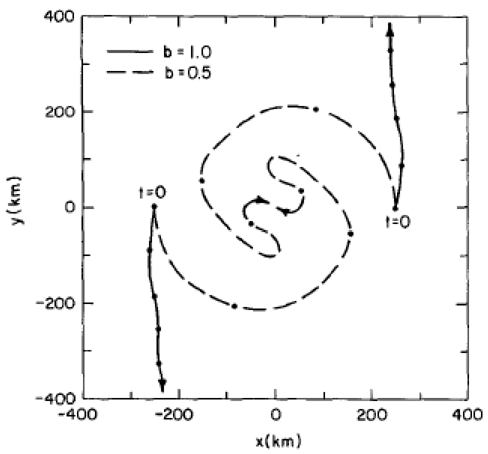

b = 1.0 drift apart

b = 0.5 merge

Binary vortex interaction

Dritschel and Waugh (1992)

【Variables】

R_1, R_2
Δ
ζ

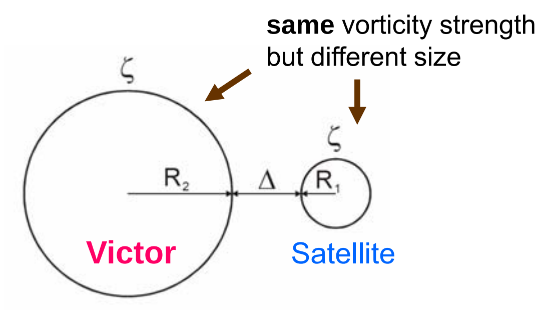

【Parameters】

- Vortex radius ratio $(r) = \frac{R_1}{R_2}$
- Dimensionless gap $(\frac{\Delta}{R_1})$

【Conclusion】

- Elastic Interaction (EI)
- Partial straining-out (PSO)
- Complete straining-out (CSO)
- Partial merger (PM)
- Complete merger (CM)

Binary vortex interaction

Kuo et al. (2004)

【Variables】

$R_1, R_2;\ \Delta;\ \zeta_1, \zeta_2$

【Parameters】

- Vortex radius ratio $(r) = \frac{R_1}{R_2}$
- Dimensionless gap $(\frac{\Delta}{R_1})$
- Vortex strength ratio $(\gamma) = \frac{\zeta_1}{\zeta_2}$

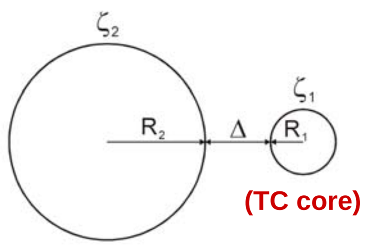

- **An extension of Dritschel and Waugh's (1992) work.**
- **In addition to the radii ratio and the normalized distance between the two vortices, the vorticity ratio is added as a third external parameters.**

CWB is capable of 24 hr and 100km scale ppn (phase locked with topography)

0 to 12 hr and 10 km ppn remain biggest challenges

355mm in 5 hr in the city of KaoShung (5 pm to 10 pm at the beginning of the rush hour)

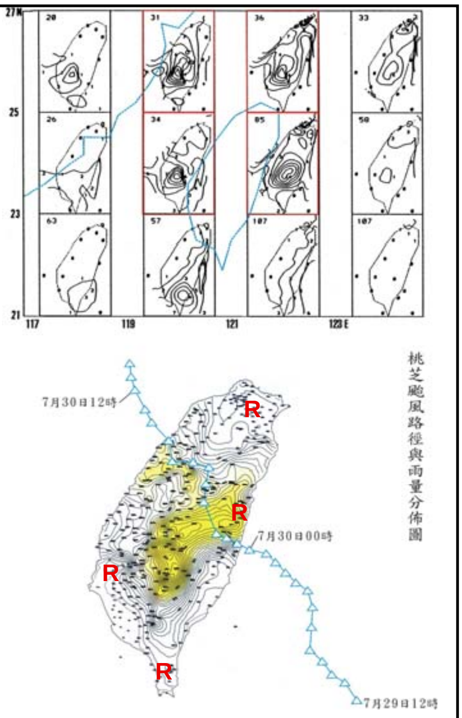

颱風潛熱與其它能量的比較

颱風的全台灣平均總雨量

為400*mm*

400 *mm* = 0.4 *m*

$0.4\ m * 1000\ kg\ m^{-3} * 2.5\times10^{6}\ J\ kg^{-1}$

$= 10^{9}\ J\ m^{2}$

$10^{9}\ J\ m^{2} * 3.5\times10^{10}\ m^{2}$

$= 3.5\times10^{19}\ J \sim 10^{20} J$

$${}^{1}_{0}n + {}^{235}_{92}U \rightarrow {}^{142}_{56}Ba + {}^{91}_{36}Kr + 3\,{}^{1}_{0}n$$

$1.68 * m * 10^{13} J/mol$

$\Rightarrow 1.46\times10^{6}\ kg\ U^{235}\ (6*10^{6}\ mol)$

能量估計值		備註
颱風降雨總潛熱能量	10^{20} J	可使台灣整層大氣增溫100度
台灣一年用電量	$5*10^{17}$ J	需數百年用電量才相當
全世界核子彈爆炸釋放能量	$2*10^{19}$ ~$2*10^{20}$ J	與颱風同等級
核戰後燃燒釋放能量	$2*10^{20}$ J	與颱風同等級
地球一天接受的太陽能量	$1.5*10^{22}$ J	數百個颱風
Tunguska隕石撞地球 （西元1908年，西伯利亞）	10^{16} J	颱風的萬分之一
火流星撞地球（恐龍滅絕？）	$4*10^{23}$ J	數千個颱風

Rozoff et al. (2006)

The strong differential rotation outside the radius of maximum wind of the core vortex may also contribute to the formation and maintenance of the moat.

The Rapid Filamentation Zone: A zone with the filamentation time smaller than the 30 min convective turnover time.

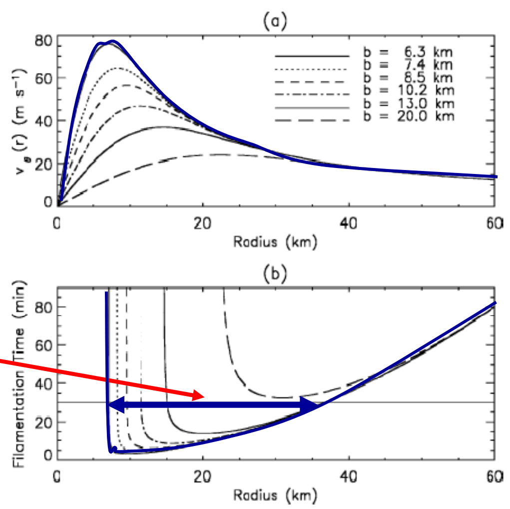

FIG. 2. (a) Radial profiles of v_θ (r) as given by (15) for six different values of the parameter b. (b) Corresponding radial profiles of $\tau_{fil}(r)$ as given by (16). The filamentation times $\tau_{fil}(r)$ are plotted only in the strain-dominated regions, where $S_1^2 + S_2^2 - \zeta^2 > 0$.

Huang and Robinson 1998

Turbulence

↑

Rhines curve

↓

Waves

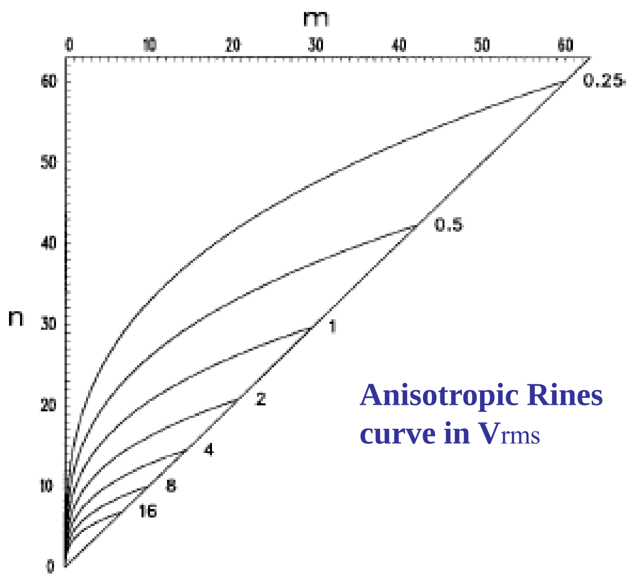

Anisotropic Rines curve in Vrms

FIG. 1. Anisotropic Rhines curve on the wavenumber plane based on Eq. (3). Dimensional values of V_{rms} (in m s^{-1}) are labeled at right.